On Orbit Performance Validation & Verification of the SMAP Instrument Antenna

Paolo Focardi and Michael W. Spencer
Jet Propulsion Laboratory, California Institute of Technology, 4800 Oak Grove Dr., Pasadena, CA 91104
Paolo.Focardi@JPL.NASA.gov

Jeffrey R. Piepmeier
Goddard Space Flight Center
8800 Greenbelt Rd, Greenbelt, MD 20771
Jeffrey.R.Piepmeier@NASA.gov

***Abstract*—NASA's Soil Moisture Active Passive (SMAP) Mission is currently flying in a 685 km orbit. Featuring a Synthetic Aperture Radar (SAR) and a radiometer sharing the same antenna, SMAP was developed in collaboration between Jet Propulsion Laboratory (JPL) and Goddard Space Flight Center (GSFC). While the radar requirements on the instrument antenna were more benign from an RF point of view, the radiometer requirement were more difficult to meet because of the stability required by the radiometer to operate to its full potential. The instrument antenna performance was predicted by a very detailed RF model and verified by measuring a 1/10th scale model with great accuracy before launch. Once in orbit, we had the opportunity to measure the antenna performance for both the radiometer and the radar and compare it with the predicted performance given by our RF model. This paper discusses the work done both at JPL and GSFC in order to verify and validate the on orbit performance of the SMAP instrument antenna.**

Keywords—on orbit performance; on orbit validation and verification; reflector antenna; offset reflector; SAR; radiometer.

I. Introduction

SMAP was launched in January 2015 and started operations after a very successful and smooth commissioning phase in April 2015. Launched into a 685 km near sun-synchronous 6AM/PM orbit, SMAP measures soil moisture on a 1000 km swath with a spatial resolution of about 40 km for the radiometer and 3 km for the radar. It measures the same area on the ground every 3 days. Early in the mission, by combining radar and radiometer data, SMAP provided 10-km resolution soil moisture data globally. Unfortunately, in July 2015 the SAR ceased its operation due to an apparent power supply failure. The radiometer, on the other hand, continues to operate smoothly and still provides high quality brightness temperature data but with a spatial resolution limited to 40 km.

Once both instruments were operational and calibrated, we were able to compare the measurements that were being made from space with predictions made using our RF model. In the next paragraph we will first describe the basic architecture of the SMAP instrument antenna and its RF model. Then we will present some of the work done at JPL to validate the performance of the radar instrument. The following paragraph will discuss the work done at GSFC on the radiometer front. In both cases the RF model was able to predict with high fidelity the performance of the antenna. Both instruments performed beautifully and produced incredibly detailed maps of soil moisture from space.

II. The SMAP Instrument Antenna

SMAP features a 6m deployable mesh reflector, in an off-set configuration, with a 4.2m focal length and boresight pointed 35.5° off from Nadir. The reflector was provided by Northrop Grumman, Astro Aerospace Division, while the feed-horn is a JPL in-house design. The dual band, dual polarization circularly-corrugated feed-horn is attached to the Spin Mechanism Assembly (SMA) along with the radiometer electronics. The feed, the boom and the reflector spin together at 14.7 rpm to cover a 1000 km swath on the ground. The radar electronics is instead inside the rectangular bus which supports the solar panels, the telecom antennas, the star tracker and all other systems. The radar is connected to the feed-horn through a rotary joint. A diplexer right behind the Ortho-Mode Transducer (OMT) is used to separate radar and radiometer signals into their respective bands.

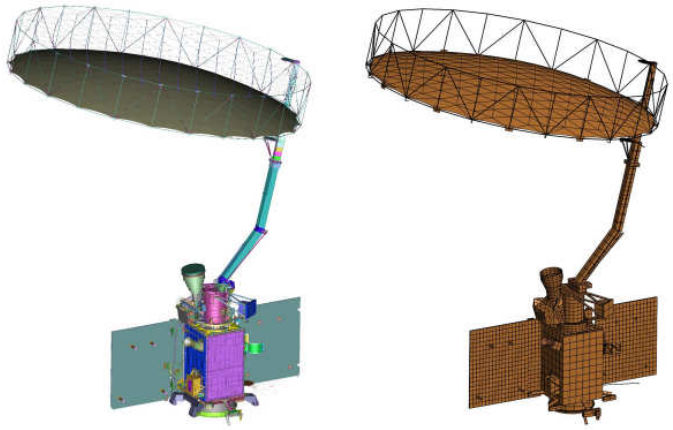

Fig. 1, Comparison between SMAP CAD (left) and RF (right) models.

Fig. 1 shows a comparison between the CAD model and the RF model. All meaningful details from an RF point of view were accounted for in the RF model. Radiation patterns were calculated every 22.5° of azimuthal rotation of the top deck.

The RF model used for performance predictions evolved over the development phases of the mission from a simple reflector and feed model to a full blown instrument and spacecraft model. The RF modeling was done mainly using GRASP™ with the PO/MoM modeling approach where PO+PTD was used for the reflector and MoM was used for the interaction with the rest of the observatory. Another RF model was also developed using HFSS™ where the feed was calculated using the FEM and the interaction with the rest of the observatory was calculated using the HFSS™ IE formulation. Both models produced accurate results and were in good agreement.

Since the top deck of the spacecraft spins at 14.7 rpm relative to the non-spinning spacecraft bus and solar panels, different radiation patterns were calculated every 22.5° of antenna rotation. The interaction of the instrument antenna with the rest of the spacecraft generated small oscillations in performance parameters that the GRASP™ model reproduced with a high level of accuracy. While the HFSS™ model was generally in good agreement with the GRASP™ model and the measurements from the scale model, it also showed small additional oscillations in gain of the order of 0.1dB. These oscillations seem to be artifacts of the HFSS™ model as they did not correlate with the geometry of the spacecraft.

A very detailed HFSS model of the feed, including waveguide-to-coax adapters, OMT, feed horn and radome, was used to generate the radiation patterns which then were fed to the GRASP™ model. Once measurements of the flight feed were available, they eventually substituted the calculations for best accuracy. Anyway, the agreement between measured and calculated radiation patterns was very good, especially within the subtended angle of the reflector for both co-pol and cx-pol at all frequencies. Small discrepancies could be observed in the feed patterns mostly in the back lobe where the flight feed was held by the positioner in the spherical range (see Fig. 2) where the measurements were performed.

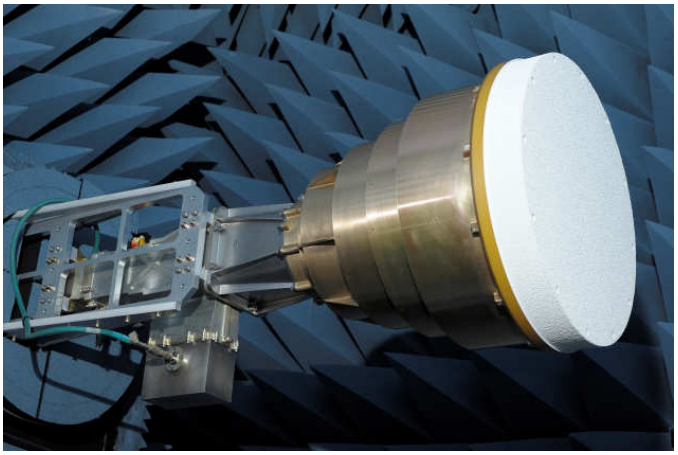

Fig. 2. SMAP Flight Feed being measured in the spherical near field range at NSI in Torrance, CA.

III. SMAP Scale Model

The 1/10th scale model was built as a means of verifying the accuracy of the RF model predictions. An RF model of the scale model was generated to capture known differences between the scale model design and the SMAP spacecraft design, as well as differences between the as-designed and as-built scale model. Some features of the scale model spacecraft, especially on the top deck and the bus, were simplified in order to make the model easier to fabricate. Those parts were mostly made of plastic and painted with a conductive paint. The machined-aluminum scale model reflector replicated the flight reflector's faceted surface design and included the truss around its rim. The boom size was increased somewhat to support the reflector and spacecraft model in the antenna range, as shown in Fig. 3. The feed horn and OMT were scaled versions of the flight feed design. In particular, the WR650 waveguide ports in the flight design were scaled down to WR62, but the waveguide-to-coax adapters at the scaled Ku-Band frequency were chosen from off-the-shelf components since scaling down the details of the actual transitions was impossible. The rest of the spacecraft was also slightly simplified in order to make it easier to fabricate, but the features that may affect the RF performance were retained.

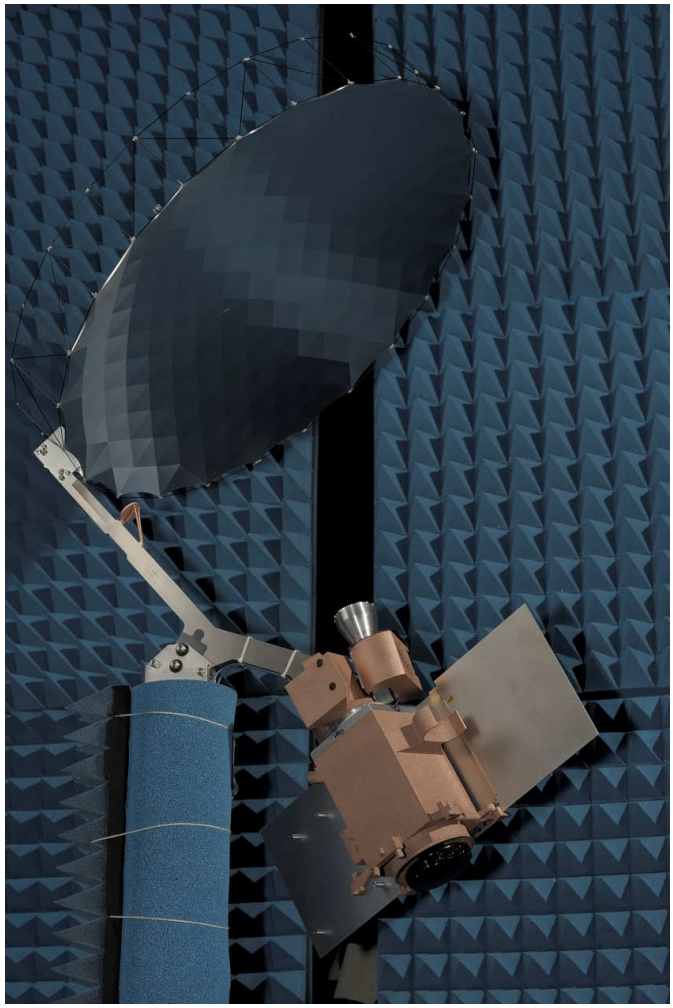

Fig. 3. SMAP 1/10th scale model in cylindrical near field antenna range at JPL.

The scale model feed was measured first, without the rest of the spacecraft. S-parameters and radiation patterns were accurately measured and both agreed very well with

predictions. Fig. 4 shows a comparison between calculated and measured return loss of the scale model feed at the OMT ports, after the WR62 waveguide-to-coax transitions were de-embedded from the measurements. This result was the first verification of the quality of the RF model and of the as-built scale model feed.

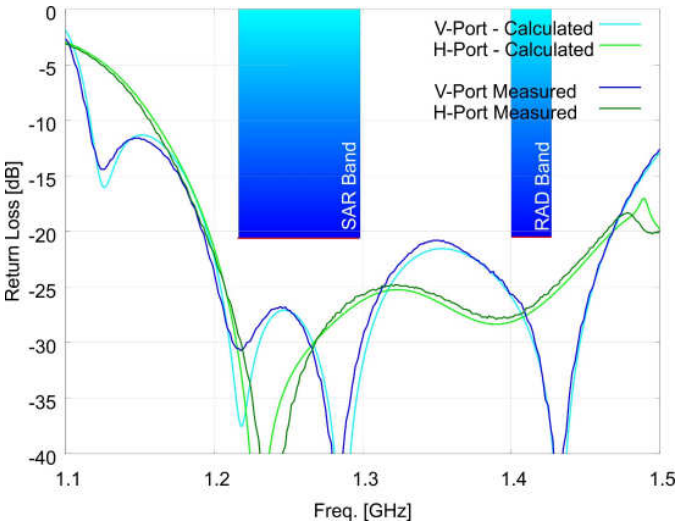

Fig. 4. Measured and calculated return loss of the scale model feed at the OMT ports after de-embedding the effect of the WR62 waveguide to coax transitions.

Once the feed performance was successfully verified, the feed was mounted on the scale model spacecraft to measure the radiation pattern of the reflector in the configuration shown in Fig. 3. The bus with the solar panels could then be clocked every 22.5° in order to simulate the spinning reflector of the flight hardware. Also, since the measurements were performed in a cylindrical range, and the full 4π steradians sphere was needed, for each position of the bus and solar panels, the model needed to be measured in two different orientations with the secondary beam pointed slightly upward and downward by 27° in order to fill the caps left blank in the cylindrical range. This angle was chosen so that the gaps in the cylindrical range ended up in areas of the pattern with very low energy to limit their importance in the overall power budget of the radiation patterns. The final pattern was then generated by the +27° case with the gaps filled by the -27° case. The final measured patterns agreed extremely well with the calculated ones.

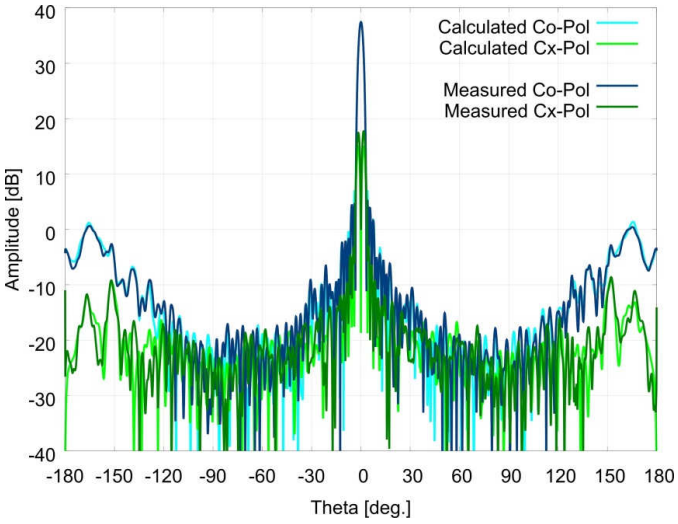

Fig. 5. Measured and calculated radiation pattern for radiometer V-pol, azimuth cut.

Fig. 5 shows an example of the excellent agreement between RF Model and scale model measurements on an azimuth cut. Every small feature of the radiation pattern was replicated with accuracy down to -60dB and -70dB from peak gain. Fig. 6 shows the elevation cut from the same data set.

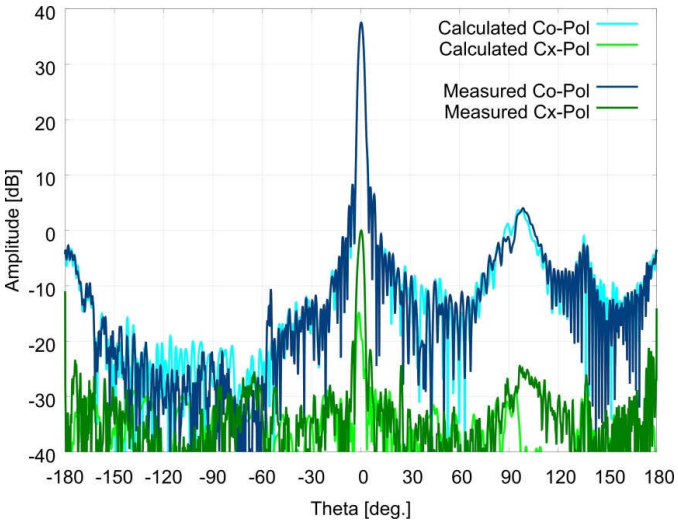

Fig. 6. Measured and calculated radiation pattern for radiometer V-pol, elevation cut.

IV. The SAR Instrument

Once in orbit, after the successful deployment of the reflector, the radar performance was assessed by examining the echoes received from Earth's surface. Fig. 7 shows an example of a comparison between the expected echo from the radar based on our RF model and the echo actually observed from the ground. The vertical axis is the received power level, scaled in amplitude and adjusted for a small pointing shift.

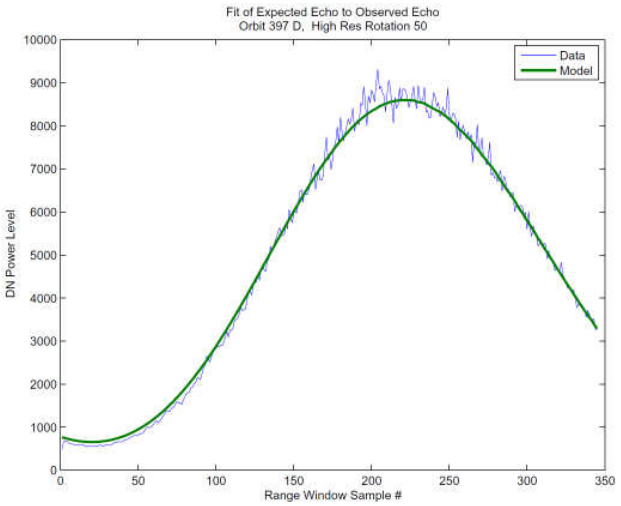

Fig. 7, Expected radar echo (green) versus measured echo (blue).

The data in Fig. 7 demonstrates that the calculated pattern does an excellent job of predicting the on-orbit performance of the antenna. In terms of pointing, the radar was expected to have a Nadir bias of 0.270° out of an allocation of 0.500°. It was actually measured to be 0.291°. A difference of just 21 milli-degrees demonstrates that all mechanical and RF systems worked well together to achieve the predicted pattern performance. Fig. 8 shows a global map of radar backscatter cross section from the SAR data.

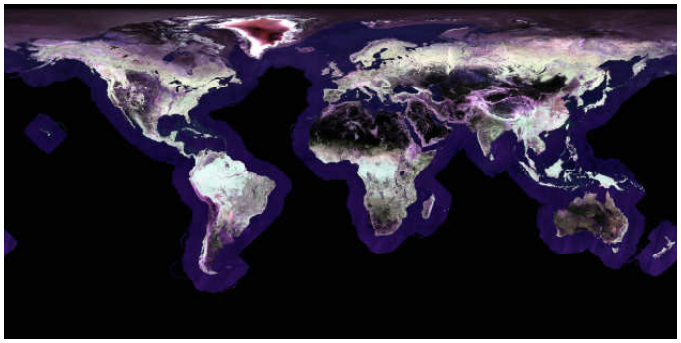

Fig. 8, Global map of radar back-scatter cross section.

V. The Radiometer Instrument

The first check of radiometer performance was done even before the reflector was deployed. With the reflector still stowed, the feed-horn had a clean view of cold space. Fig. 9 shows a comparison between the calculated and measured antenna temperature with the feed horn pointed at cold space.

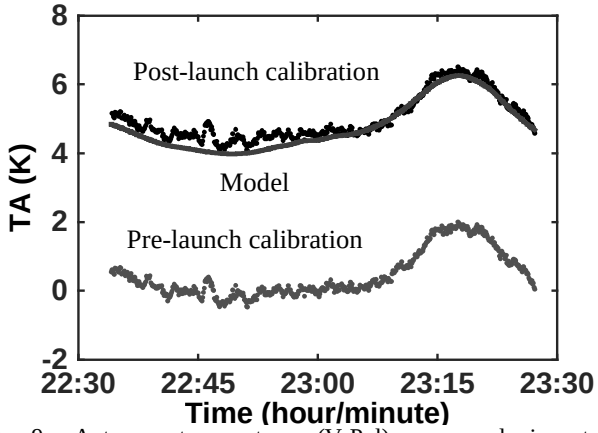

Fig. 9, Antenna temperature (V-Pol) measured in stowed configuration showing pre- (gray dots) and post-launch (black dots) calibration results compared to modeled cold-space antenna temperature (solid curve). The initial result is biased 5° K low consistent with pre-launch calibration uncertainty. H-Pol measurements showed a smaller 1° K difference.

The agreement shown in Fig. 9 is remarkable. After the deployment of the reflector the antenna pattern correction error was calculated to be of the order of 0.1%, which is about 10 times smaller than what was calculated for AQUARIUS, which measured ocean surface salinity from space.

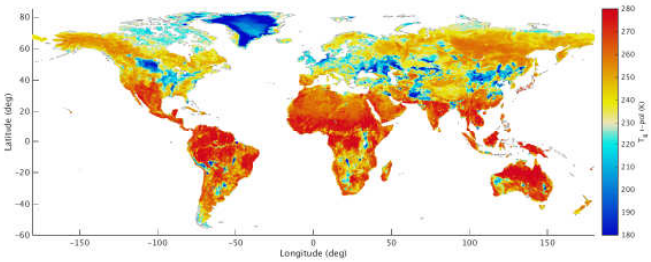

Fig. 10, SMAP brightness temperatures (H-Pol) over land from the first four days of radiometer operation (Antarctica is excluded for clarity).

The SMAP RF model predicted with great accuracy the performance of a complex instrument antenna taking into account the effect of the entire spacecraft. The increase in size and complexity of science missions combined with having reliable tools that predict antenna performance with great accuracy is enabling the design of instruments with unprecedented accuracy and resolution.

Acknowledgment

The research was carried out at the Jet Propulsion Laboratory, California Institute of Technology, under a contract with the National Aeronautics and Space Administration. A special thank goes to Jefferson A. Harrell for measuring the scale model radiation patterns. Reference herein to any specific commercial product, process, or service by trade name, trademark, manufacturer, or otherwise, does not constitute or imply its endorsement by the United States Government or the Jet Propulsion Laboratory, California Institute of Technology.